Journal of Applied Physics

Kondo effect and non-Fermi liquid behavior in metallic glasses containing Yb, Ce, and Sm

B. Huang, Y. F. Yang, and W. H. Wang

Citation: J. Appl. Phys. **113**, 163505 (2013); doi: 10.1063/1.4802660
View online: http://dx.doi.org/10.1063/1.4802660
View Table of Contents: http://jap.aip.org/resource/1/JAPIAU/v113/i16
Published by the American Institute of Physics.

JOURNAL OF APPLIED PHYSICS **113**, 163505 (2013)

Kondo effect and non-Fermi liquid behavior in metallic glasses containing Yb, Ce, and Sm

B. Huang, Y. F. Yang, and W. H. Wang[a)]
Institute of Physics, Chinese Academy of Sciences, Beijing 100190, People's Republic of China

(Received 19 March 2013; accepted 5 April 2013; published online 25 April 2013)

The low temperature properties of metallic glasses containing different concentrations of ytterbium, cerium, and samarium are studied. It is found that the Kondo effect caused by exchange interactions between the conduction and 4*f* electrons and non-Fermi liquid behavior appear in the strongly disordered alloys. We study the origins for these unique features and demonstrate that the found Kondo effect is inherited from the crystalline counterparts. The results might have significance on investigating the strong electron-electron interaction systems with structural disorder and be helpful for designing new metallic glasses with functional properties.
[http://dx.doi.org/10.1063/1.4802660]

I. INTRODUCTION

The Kondo effect reflecting the scattering of conduction electrons by magnetic moments is generally observed in crystalline alloys with a small amount of transition metals.[1] In some intermetallics containing rare earth (RE) and actinide elements, this effect has also been found which underpins a broad range of correlated electron behavior including exotic superconductivity.[2] Metallic glasses (MGs) with strongly disordered structure which is totally different from that of crystalline alloys are recent hot topics in condensed matter physics.[3–5] The Kondo effect has been discovered in series of MGs containing transition metals like amorphous Fe-Pd-Si, Co-Pd-Si, Ni-Pd-B-Cr, and Si-Mn alloys.[6–9] It is intriguing to know whether the effect is widespread in MGs containing RE elements with a 4*f* level close to the Fermi level with respect to only rare experimental data on this topic.[10] The interplay between disorder and strong electron-electron interactions in Kondo alloys is expected to be of central importance to the physics of dirty metals.[11] Experiments and calculations based on the slave-boson approach and mean field theory show that sufficient disorder can induce non-Fermi-liquid (NFL) behavior in Kondo alloys.[11–16] The NFL behavior indeed has been reported in $Ce_xLa_{65-x}Al_{10}Cu_{20}Co_5$ (x = 10, 20, and 65 at. %) MGs,[17] but the behavior has been scarcely studied yet.

In this paper, we report that the Kondo effect exists in MGs containing Yb, Ce, and Sm elements. We demonstrate that the found Kondo effect is inherited from their crystalline counterparts. NFL behavior, which is unique in Kondo alloys is also found in the glassy alloys. The NFL behavior, which is sensitive to magnetic fields and compositions, correlates closely with the competition between the Kondo effect and Ruderman-Kittel-Kasuya-Yoshida (RKKY) interactions in the strongly disordered structure.

II. EXPERIMENTS

The MGs with nominal compositions of $(CuZr)_{92.5}Al_7RE_{0.5}$ (RE = Ce, Sm, and Gd) were made with the copper mould casting method to study the microalloying effect of the RE elements on low temperature properties. CuZrAl- and Ca-based MGs with minor additions of Yb elements showed weak low temperature anomalies as most Yb elements in these MGs were nonmagnetic Yb^{2+} ions. CuZrAl-based MGs containing more Sm showed poor glass forming ability due to the positive mixing enthalpy between Zr and Sm.[18] So we chose $Yb_{12.5}Ca_{50}Zn_{20}Mg_{17.5}$, $Yb_{62.5}Zn_{15}Mg_{17.5}Cu_5$, and $Sm_{10}Y_{45}Al_{25}Co_{20}$ MGs with higher concentrations of RE elements manufactured with the induction melt-casting[8] or single-roller melt-spinning method for the studies. The fully amorphous structure of the MGs was confirmed by X-ray diffraction and differential scanning calorimeter. The measurement of resistivity, using a standard four-probe technique, was made using physical property measurement system (PPMS) 6000 of Quantum Design Company down to 1.8 K. Magnetic properties were tested in magnetic property measurement system (SQUID)-VSM 7 T System of Quantum Design Company from 1.6 K to 300 K. The measurement of heat capacity was carried out with PPMS down to 0.54 K and up to 5 T.

III. RESULTS AND DISCUSSIONS

The scaled resistivity $\rho/\rho(300\,K)$ for $Yb_{12.5}Ca_{50}Zn_{20}Mg_{17.5}$ MG at 0 T is shown in Fig. 1(a). The $\rho/\rho(300\,K)$ shows a small negative temperature coefficient at high temperatures which is typical of amorphous solids.[19] A broad peak appears around 150 K. Below the peak temperature a positive temperature coefficient appears. The change of the resistivity behavior can be explained using the extended Ziman liquid-metal theory.[20,21] If the Fermi wave number k_F is near $K_p/2$, which is the half of the first peak of structure factor, a negative temperature coefficient of the resistivity is expected as in the case of liquids. The appearance of a positive temperature coefficient at lower temperatures is caused by the change of the Fermi surface resulting in the departure of k_F from $K_p/2$. Between 30 and 100 K, the $\rho/\rho(300\,K)$ can be well fitted with the formula $\rho/\rho(0\,T, 300\,K) = \rho_{01} + B_1T - C_1T^2$ [the solid curve in Fig. 1(a)]. Below about 30 K, the resistivity deviates from the fitting curve and deceases more slowly. A minimum appears at 7.4 K. We extrapolate the

[a)]Author to whom correspondence should be addressed. Electronic mail: whw@iphy.ac.cn

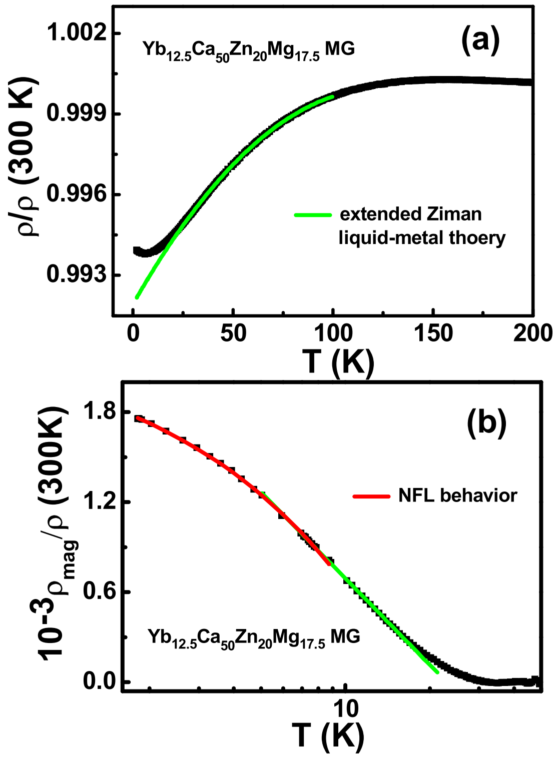

FIG. 1. (a) Temperature dependent scaled resistivity $\rho/\rho(300\,\mathrm{K})$ for $Yb_{12.5}Ca_{50}Zn_{20}Mg_{17}$ MG. The solid curve is the fitting result with the extended Ziman liquid-metal theory. (b) Temperature dependent scaled magnetic resistivity $\rho_{mag}/\rho(300\,\mathrm{K})$ in a semi-logarithmic scale for $Yb_{62.5}Zn_{15}Mg_{17.5}Cu_5$ MG. The solid lines are the fitting results.

fitting curve to 1.8 K, subtract the data from the total scaled value and obtain $\rho_{mag}/\rho(300\ \mathrm{K})$ as shown in Fig. 1(b). The $\rho_{mag}/\rho(300\ \mathrm{K})$ can be well fitted with the formula $\rho_{mag}/\rho(300\,\mathrm{K}) = \rho_{02}\text{-}A_1 lnT$ between 5.9 K and 15 K [the solid straight line in Fig. 1(b)]. The logarithmic increase of resistivity in a temperature range of about 10 K is characteristic of the Kondo effect. With the temperature decreasing conductive electrons begin to be scattered by the magnetic ions and the spin-flip process leads to the strongly temperature dependent rise of resistivity.[22] Two-level tunneling effect exists commonly in polymeric glasses and MGs.[23–26] The resistivity caused by this effect is proportional to $ln(T^2 + \Delta_1^2)$, where Δ_1 is the energy difference between the two atomic tunneling states.[27–29] The remaining appearance of the logarithmic resistivity rise for the crystallized $Yb_{12.5}Ca_{50}Zn_{20}Mg_{17.5}$ alloy excludes that the resistivity anomaly at low temperatures originates from the two-level tunneling effect.[30] The heat capacity anomalies and magnetic susceptibility sensitive to applied fields discussed below also imply the magnetic origin of the resistivity anomaly. $Yb_{62.5}Zn_{15}Mg_{17.5}Cu_5$, $(CuZr)_{92.5}Al_7RE_{0.5}$ (RE = Ce, Sm), and $Sm_{10}Y_{45}Al_{25}Co_{20}$ MGs show the similar resistivity behavior as $Yb_{12.5}Ca_{50}Zn_{20}Mg_{17.5}$ MG. With the temperature decreasing the temperature coefficients of resistivity increase and then a rapid increase of resistivity follows. We deal with the data in the same way as that for $Yb_{12.5}Ca_{50}Zn_{20}Mg_{17.5}$ MG and the fitting results are shown in Tables I and II.

The temperature dependent magnetic susceptibility χ_{total} of $Yb_{12.5}Ca_{50}Zn_{20}Mg_{17.5}$ MG was tested at 5 T. According to the Curie–Weiss law, we fit the magnetic susceptibility with the formula $\chi_{total} = \chi_{01} + cN_A\mu_0\mu_{eff}^{exp2}/[3k_B(T\text{-}\theta_p)]$, where χ_{01} is the Pauli paramagnetic susceptibility, N_A is the Avogadro's constant, μ_0 is the permeability of vacuum, k_B is the Boltzmann constant, θ_p is the Curie–Weiss temperature, c and μ_{eff}^{exp} are the atomic percentage content and effective magnetic moment of the Yb^{3+} ions, respectively.[31] The inverse magnetic susceptibility χ^{-1} ($\chi = \chi_{total}\text{-}\chi_{01}$) and the fitting lines with the Curie–Weiss law are shown in Fig. 2(a). From 100 K and 300 K, the c, μ_{eff}^{exp}, and θ_p are fitted to be 0.097%, 4.54 μ_B, and -30 K, respectively. The magnetic Yb ions in the MGs could stay in an intermediate valance state at high temperatures as those in some crystalline and quasicrystalline alloys.[32–34] The small c indicates that the intermediate valance is close to two since in sufficiently short time, the single Yb ion in metals can exhibit two valance states, nonmagnetic Yb^{2+} and magnetic Yb^{3+}.[35] Below 60 K, the susceptibility deviates from the above fitting line. This phenomenon could not be caused by crystal field effect. For Kondo alloys with crystal field effect, a broad maximum of resistivity should appear at the temperature Δ_2, which is the energy difference between two splitting energy states. A $-lnT$ relation follows at the high temperature side of the peak.[36,37] However, no such peak is found around 60 K for the studied MG. Between 20 and 30 K, the c, μ_{eff}^{exp}, and θ_p are fitted to be 0.097%, 4.00 μ_B, and -8.5 K, respectively. The reduced μ_{eff}^{exp} and $-\theta_p$ imply the screening of magnetic moments and weaker antiferromagnetic interactions.[31] The magnetic susceptibility of $Yb_{62.5}Zn_{15}Mg_{17.5}Cu_5$, $(CuZr)_{92.5}Al_7Ce_{0.5}$, $(CuZr)_{92.5}Al_7Sm_{0.5}$, and $Sm_{10}Y_{45}Al_{25}Co_{20}$ MGs all shows the similar behavior to that of $Yb_{12.5}Ca_{50}Zn_{20}Mg_{17.5}$ MG when the temperature is decreased from above 100 K to several K. The fitting results with the Curie–Weiss law are listed in Table III. According to Ref. 38, one can calculate the

TABLE I. The fitting results of the scaled resistivity with the extended Ziman liquid-metal theory for $Yb_{12.5}Ca_{50}Zn_{20}Mg_{17}$, $Yb_{62.5}Zn_{20}Mg_{17.5}Cu_5$, $(CuZr)_{92.5}Al_7RE_{0.5}$ (X = Ce, Sm), and $Sm_{10}Y_{45}Al_{25}Co_{20}$ MGs.

MG	Temperature range (K)	ρ_{01}	B_1 (10^{-4} K^{-1})	C_1 (10^{-7} K^{-2})
$Yb_{12.5}Ca_{50}Zn_{20}Mg_{17.5}$	30–100	0.992	1.300	−5.289
$Yb_{62.5}Zn_{20}Mg_{17.5}Cu_5$	50–100	1.021	0	−4.031
$(CuZr)_{92.5}Al_7Ce_{0.5}$	15–50	1.037	−0.648	−10.69
$(CuZr)_{92.5}Al_7Sm_{0.5}$	15–50	1.040	−1.401	−5.362
$Sm_{10}Y_{45}Al_{25}Co_{20}$	30–50	1.057	−1.360	−7.899

TABLE II. The fitting results of the scaled magnetic resistivity $\rho_{mag}/\rho(300\,\mathrm{K})$ at low temperatures with the formula $\rho_{mag}/\rho(300\,\mathrm{K}) = \rho_{02}\text{-}A_1 lnT$ for $Yb_{12.5}Ca_{50}Zn_{20}Mg_{17}$, $Yb_{62.5}Zn_{20}Mg_{17.5}Cu_5$, $(CuZr)_{92.5}Al_7RE_{0.5}$ (X = Ce, Sm), and $Sm_{10}Y_{45}Al_{25}Co_{20}$ MGs.

MG	Temperature range (K)	ρ_{02}(10^{-3})	A_1 (10^{-3})
$Yb_{12.5}Ca_{50}Zn_{20}Mg_{17.5}$	5.9–15.0	2.60	0.83
$Yb_{62.5}Zn_{20}Mg_{17.5}Cu_5$	3.4–12.5	9.28	3.02
$(CuZr)_{92.5}Al_7Ce_{0.5}$	2.1–8.8	0.94	0.42
$(CuZr)_{92.5}Al_7Sm_{0.5}$	2.1–8.8	1.17	0.51
$Sm_{10}Y_{45}Al_{25}Co_{20}$	4.0–9.9	8.98	3.42

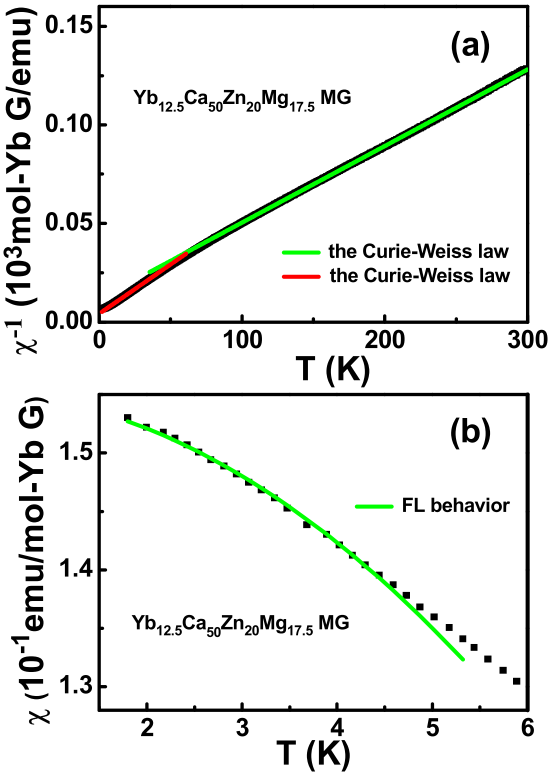

FIG. 2. (a) Temperature dependent inverse magnetic susceptibility χ^{-1} for $Yb_{12.5}Ca_{50}Zn_{20}Mg_{17}$ MG. The solid lines are the fitting results with the Curie-Weiss law at different temperatures. (b) Temperature dependent magnetic susceptibility χ for $Yb_{12.5}Ca_{50}Zn_{20}Mg_{17}$ MG. The solid curve is the fitting result within the local FL theory.

theoretical effective magnetic moments μ_{eff}^{theo} of Yb^{3+}, Sm^{3+}, Ce^{3+} ions, which are also listed in Table III to compare with the fitted values of μ_{eff}^{exp} for these MGs containing Yb, Sm, and Ce.[38] The magnetic susceptibility for $Sm_{10}Y_{45}Al_{25}Co_{20}$ MG can be properly fitted with the Curie-Weiss law at high temperatures with μ_{eff}^{exp} equaling to 0.69 μ_B/f. u. which is close to the theoretical value μ_{eff}^{theo} 0.84 μ_B/f. u.[38] The absence of Van Vleck contribution at high temperatures for $Sm_{10}Y_{45}Al_{25}Co_{20}$ MG imply the weak crystal electric fields in the amorphous alloys perhaps due to the nearly spherical environment around the RE ions.[39,40]

TABLE III. The fitting results of the magnetic susceptibility with the Curie-Weiss law in different temperature ranges for $Yb_{12.5}Ca_{50}Zn_{20}Mg_{17}$, $Yb_{62.5}Zn_{20}Mg_{17.5}Cu_5$, $(CuZr)_{92.5}Al_7RE_{0.5}$ (X = Ce, Sm), and $Sm_{10}Y_{45}Al_{25}Co_{20}$ MGs.

MG	Temperature range (K)	c (%)	$\mu_{eff}^{exp}(\mu_B/f.u.)$	$\mu_{eff}^{theo}(\mu_B/f.u.)$	$\theta_p(K)$
$Yb_{12.5}Ca_{50}Zn_{20}Mg_{17}$	200–300	0.097	4.54	4.54	−30
	20–30	0.097	4.00	4.54	−8.5
$Yb_{62.5}Zn_{20}Mg_{17.5}Cu_5$	200–300	0.488	4.54	4.54	−20
	20–30	0.488	4.04	4.54	−3.9
$(CuZr)_{92.5}Al_7Ce_{0.5}$	100–275	0.5	1.49	2.54	−45
	20–30	0.5	1.20	2.54	−9.0
$(CuZr)_{92.5}Al_7Sm_{0.5}$	50–70	0.5	0.49	0.84	−15
	20–30	0.5	0.44	0.84	−1.2
$Sm_{10}Y_{45}Al_{25}Co_{20}$	100–170	10	0.69	0.84	−41
	20–30	10	0.53	0.84	−3.1

TABLE IV. The fitting results of the magnetic susceptibility χ with the formula $\chi = \chi_{02}(1 - C_2T^2)$ at low temperatures under a magnetic field of 5 T for $Yb_{12.5}Ca_{50}Zn_{20}Mg_{17}$, $Yb_{62.5}Zn_{20}Mg_{17.5}Cu_5$, and $(CuZr)_{92.5}Al_7Ce_{0.5}$ MGs.

MG	Magnetic field (T)	Temperature range (K)	χ_{02} (0.1 emu mol Yb G)
$Yb_{12.5}Ca_{50}Zn_{20}Mg_{17}$	5	1.8–4.4	1.55
$Yb_{62.5}Zn_{20}Mg_{17.5}Cu_5$	5	1.6–3.0	2.40
$(CuZr)_{92.5}Al_7Ce_{0.5}$	5	1.9–3.6	0.36

The magnetic susceptibility of $Yb_{12.5}Ca_{50}Zn_{20}Mg_{17.5}$ MG between 1.8 K and 4.4 K under a field of 5 T can be fitted by $\chi = \chi_{02}(1\text{-}C_2T^2)$ as shown in Fig. 2(b). The behavior is the feature of Kondo alloys.[1] The large Pauli magnetic susceptibility χ_{02} (0.155 emu/mol-Yb) obtained from the fitting is contributed by the strongly renormalized quasiparticles described by the local FL theory.[41] The magnetic susceptibilities of $Yb_{62.5}Zn_{15}Mg_{17.5}Cu_5$ and $(CuZr)_{92.5}Al_7Ce_{0.5}$ MGs at 5 T also show the $-T^2$ relation at low temperatures. The fitting results are listed in Table IV.

With the formula $\mu_{sat}^{theo} = [J/(J+1)]^{1/2}\mu_{eff}^{theo}$, where J is the total angular momentum at the ground state, the theoretical saturated magnetic moment μ_{sat}^{theo} of Yb^{3+} ions is calculated to be 4.00 μ_B.[31] The saturated magnetic moment per Yb^{3+} ion at 7 T and 1.8 K for $Yb_{12.5}Ca_{50}Zn_{20}Mg_{17.5}$ MG is tested as 1.83 μ_B, which is much smaller than the theoretical value. As listed in Table V, the experimental saturated magnetic moments μ_{sat}^{exp} of $Yb_{62.5}Zn_{15}Mg_{17.5}Cu_5$, $(CuZr)_{92.5}Al_7RE_{0.5}$ (RE = Ce, Sm), and $Sm_{10}Y_{45}Al_{25}Co_{20}$ MGs are all much smaller than the theoretical values. This behavior is different from that of $(CuZr)_{92.5}Al_7Gd_{0.5}$ MG which does not show the Kondo effect. Excluding the influence of crystal field effect the reduced experimental saturated magnetic moments could be due to the Kondo screening effect.

The specific heat for $Yb_{12.5}Ca_{50}Zn_{20}Mg_{17.5}$ MG between 5 K and 10 K at 0 T can be fitted with the conventional formula $C_p/T = \gamma + \beta T^2$ for metals[31] and deviation occurs below about 3 K as shown in Fig. 3(a). We subtract the extrapolated specific heat calculated with $C_p = \gamma T + \beta T^3$ from the total specific heat, scale the result with the concentration of Yb^{3+} ions at high temperatures and obtain the abnormal specific heat ΔC_p. The ΔC_p for $Yb_{12.5}Ca_{50}Zn_{20}Mg_{17.5}$ MG at 0 T and 5 T are shown in Fig. 3(b). A broad peak appears

TABLE V. The experimental saturated magnetic moments μ_{sat}^{exp} for $Yb_{12.5}Ca_{50}Zn_{20}Mg_{17}$, $Yb_{62.5}Zn_{20}Mg_{17.5}Cu_5$, $Sm_{10}Y_{45}Al_{25}Co_{20}$, and $(CuZr)_{92.5}Al_7X_{0.5}$ (X = Ce, Sm, and Gd) MGs at low temperatures and high fields.

MG	Temperature (K)	Magnetic field (T)	μ_{sat}^{exp} $(\mu_B/f.u.)$	μ_{sat}^{theo} $(\mu_B/f.u.)$
$Yb_{12.5}Ca_{50}Zn_{20}Mg_{17}$	1.8	7	1.83	4.00
$Yb_{62.5}Zn_{20}Mg_{17.5}Cu_5$	1.6	7	2.35	4.00
$(CuZr)_{92.5}Al_7Ce_{0.5}$	1.6	7	0.40	2.14
$(CuZr)_{92.5}Al_7Sm_{0.5}$	1.6	5	0.21	0.71
$Sm_{10}Y_{45}Al_{25}Co_{20}$	1.6	7	0.09	0.71
$(CuZr)_{92.5}Al_7Gd_{0.5}$	1.6	7	6.86	7.00

around 1.83 K under a magnetic field of 0 T. Between 0.54 K and 1.13 K, ΔC_p can be fitted with $\Delta C_p = \Delta C_{p0} + \gamma_e T$ in which ΔC_{p0} and γ_e equal to 0.25 J/mol-Yb K and 0.210 J/mol-Yb K^2 [the solid straight line in Fig. 3(b)]. The small constant ΔC_{p0} could be contributed by magnetic clusters.[42] The large electronic specific heat coefficient γ_e indicates moderate heavy FL behavior.[2] We linearly extrapolate the ΔC_p at 0 T to 0 K and calculate the entropy change with the formula $\Delta S(T) = \int_0^T \Delta C_p/TdT$. The ΔS (3.5 K) reaches 89% of $Rln2$, i.e., 5.10 J/mol-Yb K [the soild curve in Fig. 3(b)]. The ΔC_p corresponds to the compensation of the ground state of Yb^{3+} ($4f^{13}$) with a spin quantum number $S = 1/2$ indicating the absence of crystal field effect at higher temperatures.[42] Under 5 T, the ΔC_p peak moves to a higher temperature with a larger peak value. The magnetic field energy is greater than the binding energy of free electrons and Zeeman splitting of the ground state modifies the abnormal specific heat peak.[1] The features of ΔC_p for $Yb_{12.5}Ca_{50}Zn_{20}Mg_{17.5}$ MG strongly favor that Kondo effect appears in this MG. Similar specific heat anomalies also appear for $(CuZr)_{92.5}Al_7RE_{0.5}$ (RE = Ce, Sm) MGs.

The Schottky effect is common in crystalline alloys and could induce the anomalies of low temperature properties.[22] The $(CuZr)_{92.5}Al_7Gd_{0.5}$ MG has typical Schottky anomalies which show different features with the Kondo effect.[43] For this MG with increasing applied fields or decreasing temperatures more magnetic moments will stay at low energy states and have larger projections in the direction of magnetic fields. Accordingly the magnetization will increase and the

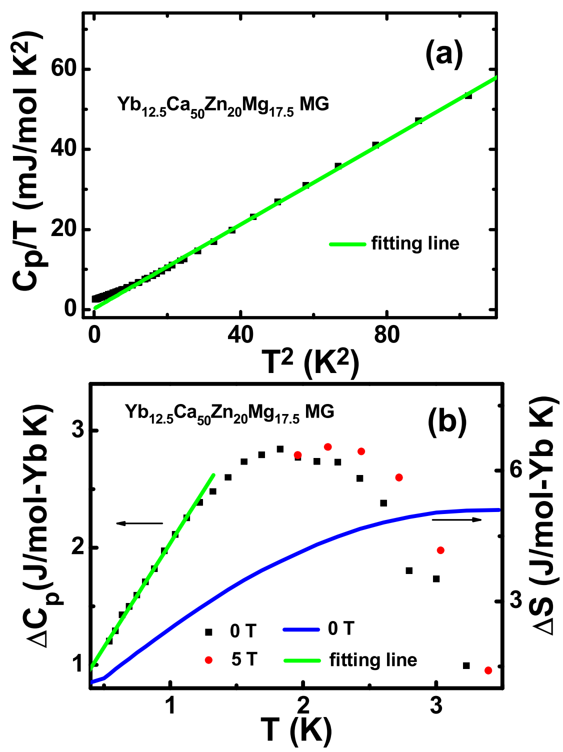

FIG. 3. (a) Temperature scaled heat capacity C_p/T vs. T^2 for $Yb_{12.5}Ca_{50}Zn_{20}Mg_{17}$ MG. The solid line is fitting result with $C_p/T = \gamma + \beta T^2$. (b) Temperature dependent abnormal ΔC_p for $Yb_{12.5}Ca_{50}Zn_{20}Mg_{17}$ MG at 0 T and 5 T. The solid straight line is the fitting result. The solid curve presents the T dependant entropy change ΔS at 0 T.

magnetic susceptibility $\chi = M/H$ will decrease. So the inverse magnetic susceptibility χ^{-1} shows an upturn deviation from the Curie-Weiss law with decreasing temperatures and the deviation becomes more obvious under a higher magnetic field. For the Kondo effect χ^{-1} often shows a down turn deviation from the Curie-Weiss law due to weaker antiferromagnetic interactions as shown in Fig. 2(a). Schottky effect will not cause the logarithmic increase of the resistivity which is characteristic of Kondo effect. Besides, the specific heat anomalies contributed by the two effects are also quite different. Specific heat contributed by the Schottky effect approaches zero exponentially at the low temperature side while at high temperatures the specific heat varies as T^{-2}.[42] For Kondo effect a broad specific heat peak appears with a linear relation of the temperature at the low temperature side.[1] The typical features of $Yb_{12.5}Ca_{50}Zn_{20}Mg_{17.5}$, $Yb_{62.5}Zn_{15}Mg_{17.5}Cu_5$, $(CuZr)_{92.5}Al_7RE_{0.5}$ (RE = Ce, Sm), and $Sm_{10}Y_{45}Al_{25}Co_{20}$ MGs discussed previously are unequivocally caused by Kondo effect rather than the Schottky effect.

In a single impurity Kondo system, k_BT_K reflecting the binding energy of the singlet ground state is proportional to $\exp[-|E_F\text{-}E_f|/N(E_F)V_{k,f}{}^2]$, where E_f and E_F are, respectively, the energies of the f level and Fermi level, $N(E_F)$ is the conduction-band density of states at the Fermi level, $V_{k,f}$ is the hybridization matrix between the f state and the conduction electrons.[1] In MGs, the nearest-neighbor distance has a considerable distribution which results in the distribution in the f levels,[44,45] and thus the distribution of the Kondo temperature T_K. The Kondo specific heat peak appears near T_K conventionally.[1] From the specific heat anomalies of $Yb_{12.5}Ca_{50}Zn_{20}Mg_{17.5}$, $(CuZr)_{92.5}Al_7RE_{0.5}$ (RE = Ce, Sm) MGs we find that the T_K distribute mainly around 2 K for the MGs. According to the analysis of the magnetic susceptibility, when the temperature is deceased the change of states $4f^{13} \to 4f^{14}$, $4f^1 \to 4f^0$, and $4f^5 \to 4f^6$ occurs for the MGs containing Yb, Ce, and Sm, respectively.[38] Actually, with the decreasing temperature Kondo effect corresponding to the delocalization (for Ce) or localization (for Yb and Sm) of $4f$ electrons has been reported to exist in many crystalline alloys like $YbCu_5$, $YbNiAl_2$, $CeCu_6$, $CeCu_2Si_2$, $(LaSm)Sn_3$, and so on.[46–49] For these alloys, the T_K range from a few to tens of Kelvin. The existence of Kondo effect in MGs containing Yb, Ce, and Sm elements indicates the inheritance of electronic structures. In these MGs when the metallic atoms approach each other, the short-range interactions among them, which are similar to those of their crystalline counterparts, split the energy levels of the atoms and form the conduction and $4f$ energy bands.[31] The lack of long-range order mainly influences the density of the energy states and the property of the eigenstates.[50,51] The $4f$ energy levels in the MGs are still close to the Fermi surface and the Kondo effect still exists when the temperature is decreased. Recently, the inheritance of elastic properties and polyamorphic phase transitions from the solvent components has been discovered for MGs and a hierarchy of atomic bands is suggested.[52–54] As Kondo effect mainly relates with the interaction between the magnetic atoms and their neighboring ligands, this effect is inherited even though the magnetic atoms act as solute components in our studied MGs.

Next, we will show that due to the disordered packing of various atoms the NFL behavior, which is unique in crystalline Kondo alloys is found in our studied MGs. According to the Landau's FL theory, the magnetic susceptibility and resistivity of Kondo alloys should have a T^2 term, and the specific heat should decrease linearly when the temperature approaches zero.[41] For $Yb_{12.5}Ca_{50}Zn_{20}Mg_{17.5}$ MG the magnetic susceptibility χ_{total} between 1.8 and 9.9 K at 0.1 T can be fitted with the formula $\chi_{total} = \chi_{03} + C_3T^{-1+\alpha}$ in which α equals to 0.337. The temperature dependent $\Delta\chi$ ($\Delta\chi = \chi_{total} - \chi_{03}$) and fitting line are shown in Fig. 4(a). The scaled magnetic resistivity of the MG between 1.8 K and 7.9 K without fields can be fitted with the formula $\rho_{mag}/\rho(300\,\mathrm{K}) = \rho_{03} + A_2T^{\lambda}$ with λ equaling to 0.644 [the solid curve in Fig. 1(b)]. $\Delta C_p/T$ at 0 T is approximately proportional to $-lnT$ between 2.1 K and 3.7 K. It is difficult to get

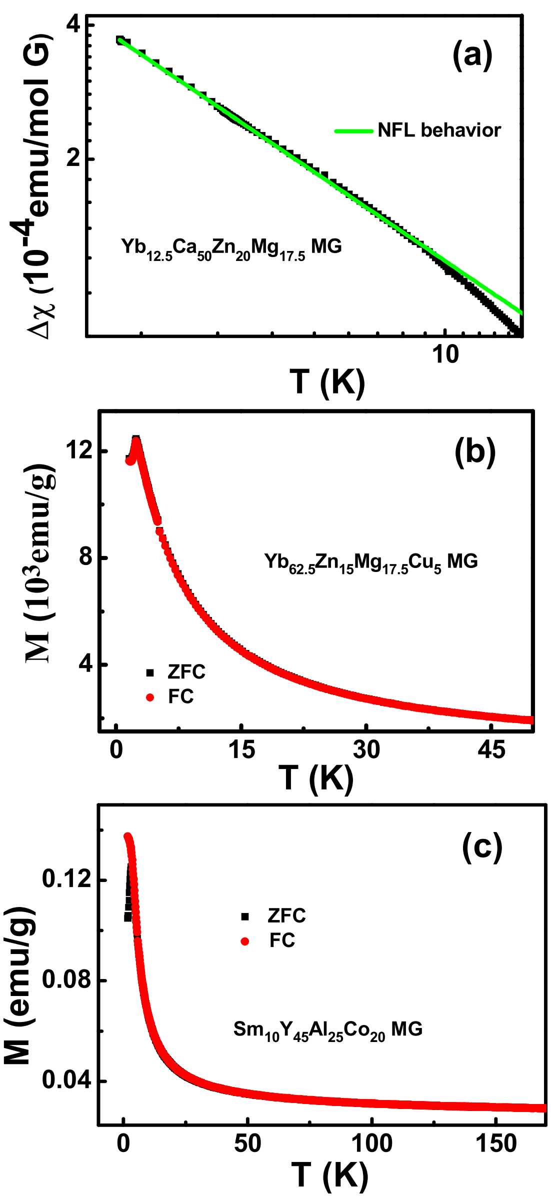

FIG. 4. (a) Temperature dependent magnetic susceptibility $\Delta\chi$ for $Yb_{12.5}Ca_{50}Zn_{20}Mg_{17}$ MG in a logarithmic scale. The solid line is the fitting result with the NFL theory. (b) Temperature dependent ZFC and FC magnetization M for $Yb_{62.5}Zn_{15}Mg_{17}Cu_5$ MG at 0.1 T. (c) Temperature dependent ZFC and FC magnetization M for $Sm_{10}Y_{45}Al_{25}Co_{20}$ MG at 1 T.

TABLE VI. The fitting results of the magnetic susceptibility with the formula $\chi_{total} = \chi_{03} + C_3T^{-1+\alpha}$ at low temperatures and different fields for $Yb_{12.5}Ca_{50}Zn_{20}Mg_{17}$ and $(CuZr)_{92.5}Al_7RE_{0.5}$ (X = Ce, Sm) and MGs.

MG	Magnetic field (T)	Temperature range (K)	α
$Yb_{12.5}Ca_{50}Zn_{20}Mg_{17.5}$	0.1	1.8–9.9	0.337
$(CuZr)_{92.5}Al_7Ce_{0.5}$	0.5	1.6–10.2	0.394
$(CuZr)_{92.5}Al_7Sm_{0.5}$	1	1.6–9.8	0.106
$(CuZr)_{92.5}Al_7Sm_{0.5}$	5	1.6–9.7	0.335

the small magnetic contribution to specific heat above 3.7 K due to the mixing with the boson peak originating from low frequency vibration modes.[55] The deviation from the FL theory in a large temperature range indicates the existence of NFL behavior in $Yb_{12.5}Ca_{50}Zn_{20}Mg_{17.5}$ MG.[15] The temperature dependent magnetic susceptibility of $(CuZr)_{92.5}Al_7RE_{0.5}$ (RE = Ce, Sm) MGs also shows the NFL behavior.

The fitting results of the magnetic susceptibility at low temperatures with the formula $\chi_{total} = \chi_{03} + C_3T^{-1+\alpha}$ for $Yb_{12.5}Ca_{50}Zn_{20}Mg_{17.5}$ and $(CuZr)_{92.5}Al_7RE_{0.5}$ (RE = Ce, Sm) MGs are listed in Table VI. For $(CuZr)_{92.5}Al_7Sm_{0.5}$ MG, α increases from 0.106 to 0.335 when the field increases from 1 T to 5 T. For $(CuZr)_{92.5}Al_7Ce_{0.5}$ and $Yb_{12.5}Ca_{50}Zn_{20}Mg_{17.5}$ MGs when the applied field increases to 5 T, the NFL behavior disappears and local FL behavior exists as listed in Table IV. For $Yb_{62.5}Zn_{15}Mg_{17.5}Cu_5$ and $Sm_{10}Y_{45}Al_{25}Co_{20}$ MGs containing larger concentrations of RE elements the NFL behavior also disappears. The overlapped zero field cooled (ZFC) and field cooled (FC) magnetization curves at 0.1 T show sharp antiferromagnetic peaks at 2.40 K for $Yb_{62.5}Zn_{15}Mg_{17.5}Cu_5$ MG as shown in Fig. 4(b). For $Sm_{10}Y_{45}Al_{25}Co_{20}$ MG, the ZFC and FC magnetization curves at 1 T show a rapid increase around 6 K and then bifurcate at 3.75 K indicating a spin glass transition as shown in Fig. 4(c).[56] The NFL behavior of MGs containing Yb, Ce, and Sm elements can be affected by the applied magnetic fields and concentrations of the RE elements.

The competition between the Kondo effect and RKKY interactions in the disordered structures induces the NFL behavior. Either of the two competing tendencies would dominate due to the large spatial fluctuations in the MGs. In the region where the distances between the magnetic moments are sufficiently large RKKY interactions are very weak and a disordered local FL forms at low temperatures through the Kondo effect. On the other hand, ferromagnetic, antiferromagnetic, or spin glass clusters form through RKKY interactions in the regions where the concentrations of magnetic moments are high. The broad distribution of Kondo temperatures T_K in various regions with comparable energies of Kondo effect and RKKY interactions directly results in the NFL behavior.[11–13] Fig. 5(a) illustrates the distribution and interactions among the RE magnetic spins under a small field at low temperatures. Darker color means stronger RKKY interactions. In the picture, T_K distribute in a large temperature range due to the spatial fluctuations and NFL behavior exists. If the temperature is lower than all the T_K in different areas local FL liquid forms just as the heat capacity behavior for $Yb_{12.5}Ca_{50}Zn_{20}Mg_{17.5}$ MG below 1.13 K. So the ground state of this MG

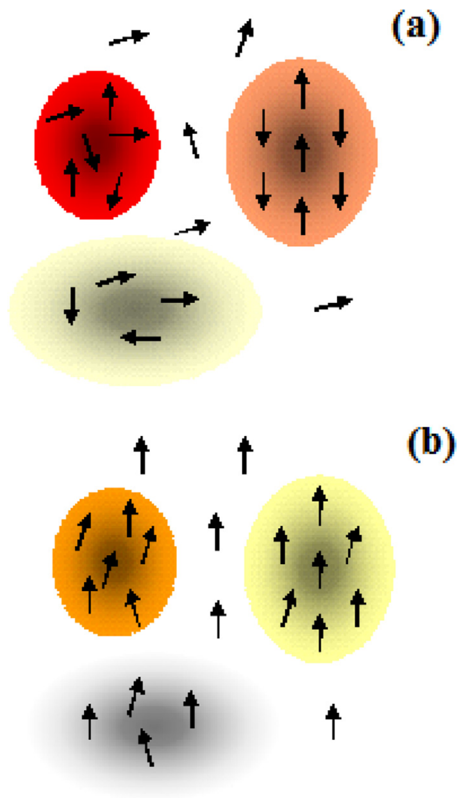

FIG. 5. (a) The distribution and interactions of the RE magnetic spins under a small magnetic field. (b) The distribution and interactions of the RE magnetic spins under a high magnetic field. The direction of the field is up.

at small fields is not the NFL states. Within the statistical dynamical mean field theory the exponent α is a continuously varying function of the disorder strength and a less disordered structure with a narrower T_K distribution corresponds to a larger α.[15] Under a high magnetic field the tendency for the spins to arrange along the direction of the applied field becomes more pronounced and the magnetic ions seem to stay in a more ordered structure and the T_K distribution becomes narrower. Increased α for $(CuZr)_{92.5}Al_7Sm_{0.5}$ MG at a higher magnetic field coincides with the prediction. Under sufficient large fields the antiferromagnetic temperatures T_N or freezing temperatures T_f approaches zero[31,56,57] and RKKY interactions seem to be very weak. The largely weakened RKKY interactions and narrow T_K distribution lead to the disappearance of the NFL behavior for $(CuZr)_{92.5}Al_7Ce_{0.5}$ and $Yb_{12.5}Ca_{50}Zn_{20}Mg_{17.5}$ MGs under high magnetic fields. Fig. 5(b) illustrates the distribution and interactions of the RE magnetic spins under a high field. The direction of the applied field is up. Local FL forms in more areas with weak RKKY interactions. With increasing concentrations of Sm and Yb in MGs RKKY interactions become stronger and the spin-flip processes of Kondo effect are suppressed. The NFL behavior disappears and the antiferromagnetic and spin glass transitions exist for $Yb_{62.5}Zn_{15}Mg_{17.5}Cu_5$ and $Sm_{10}Y_{45}Al_{25}Co_{20}$ MGs, respectively.

IV. CONCLUSIONS

We find that Kondo effect exists in MGs containing Yb, Ce, and Sm unequivocally. The NFL behavior sensitive to magnetic fields and concentrations, which is unique in Kondo alloys and MGs is discovered. The phenomenon can be explained with the competition between the Kondo effect and RKKY interactions in the strongly disordered structure. We also show that the origins for these unique features and the found Kondo effect of these MGs is inherited from their crystalline counterparts, and the inheritance of electronic structure has significance for the exploring of MGs with functional properties. Kondo effect underpins a variety of interesting physical phenomena like exotic superconductivity and anomalous ground states. The found MGs with Kondo effect could provide models for the study of the influence of disorder on strong electron-electron interactions.

ACKNOWLEDGMENTS

The financial support was from the NSF of China (Grant Nos. 51271195 and 50921091). We thank P. J. Sun, D. Q. Zhao, D. W. Ding, P. Wen, and S. K. Su for the experimental assistance and helpful discussions.

[1] A. C. Hewson, *The Kondo Problem to Heavy Fermions* (Cambridge University Press, Cambridge, 1993).
[2] G. R. Stewart, Rev. Mod. Phys. **56**, 755 (1984).
[3] B. C. Wei, Y. Zhang, M. X. Pan, and W. H. Wang, J. Appl. Phys. **89**, 3529 (2001).
[4] W. H. Wang, Prog. Mater. Sci. **52**, 540 (2007).
[5] W. H. Wang, Prog. Mater. Sci. **57**, 487 (2012).
[6] C. C. Tsuei and R. Hasegawa, Solid State Commun. **7**, 1581 (1969).
[7] R. Hasegawa and C. C. Tsuei, Phys. Rev. B **3**, 214 (1971).
[8] V. K. C. Liang and C. C. Tsuei, Phys. Rev. B **7**, 3215 (1973).
[9] A. I. Yakimov, A. V. Dvurechenskii, C. J. Adkins, and V. A. Dravin, J. Phys. Condens. Matter **9**, 499 (1999).
[10] T. Hihara, K. Sumiyama, H. Yamauchi, Y. Homma, T. Suzuki, and K. Suzuki, J. Phys. Condens. Matter **5**, 8425 (1999).
[11] V. Dobrosavljević, T. R. Kirkpatrick, and G. Kotliar, Phys. Rev. Lett. **69**, 1113 (1992).
[12] E. Miranda, V. Dobrosavljević, and G. Kotliar, Phys. Rev. Lett. **78**, 290 (1997).
[13] A. H. C. Neto, G. Castilla, and B. A. Jones, Phys. Rev. Lett. **81**, 3531 (1998).
[14] G. R. Stewart, Rev. Mod. Phys. **73**, 797 (2001).
[15] E. Miranda and V. Dobrosavljević, Rep. Prog. Phys. **68**, 2337 (2005).
[16] G. R. Stewart, Rev. Mod. Phys. **78**, 743 (2006).
[17] M. B. Tang, H. Y. Bai, W. H. Wang, D. Bogdanov, K. Winzer, K. Samwer, and T. Egami, Phys. Rev. B **75**, 172201 (2007).
[18] A. Takeuchi and A. Inoue, Mater. Trans. **46**, 2817 (2005).
[19] R. Zallen and J. Wiley, *The Physics of Amorphous Solids* (Wiley Online Library, 1983).
[20] P. J. Cote and L. V. Meisel, Phys. Rev. Lett. **39**, 102 (1977).
[21] S. R. Nagel, Phys. Rev. B **16**, 1694 (1977).
[22] C. Enss and S. Hunklinger, *Low-Temperature Physics* (Springer, Berlin, 2005).
[23] M. Banville and R. Harris, Phys. Rev. Lett. **44**, 1136 (1980).
[24] D. A. Parshin, X. Liu, O. Brand, and H. van Lohneysen, Z. Phys. B **93**, 57 (1993).
[25] A. Brodin, A. Fontana, L. Börjesson, G. Carini, and L. M. Torell, Phys. Rev. Lett. **73**, 2067 (1994).
[26] D. A. Parshin, Phys. Rev. B **49**, 9400 (1994).
[27] R. W. Cochrane, R. Harris, J. O. Strom-Olson, and M. J. Zuckermann, Phys. Rev. Lett. **35**, 676 (1975).
[28] H. Y. Bai, C. Z. Tong, and P. Zheng, J. Appl. Phys. **95**, 1269 (2004).
[29] M. B. Tang, H. Y. Bai, M. X. Pan, D. Q. Zhao, and W. H. Wang, J. Non-Cryst. Solids **351**, 2572 (2005).
[30] R. W. Cochrane and J. O. Strom-Olsen, J. Phys. F: Met. Phys. **7**, 1799 (2001).
[31] C. Kittel, *Introduction to Solid State Physics*, 7th ed. (John Wiley & Sons, New York, 1996).
[32] V. H. Tran, W. Miller, A. Kowalczyk, T. Tolinski, and G. Chelkowska, J. Phys.: Condens. Matter **18**, 10353 (2006).

[33]K. Kummer, Y. Kucherenko, S. Danzenbacher, C. Krellner, C. Geibel, M. G. Holder, L. V. Bekenov, T. Muro, Y. Kato, T. Kinoshita, S. Huotari, L. Simonelli, S. L. Molodtsov, C. Laubschat, and D. V. Vyalikh, Phys. Rev. B **84**, 245114 (2011).
[34]T. Watanuki, S. Kashimoto, D. Kawana, T. Yamazaki, A. Machida, Y. Tanaka, and T. J. Sato, Phys. Rev. B **86**, 094201 (2012).
[35]D. Kaczorowski, A. Leithe-Jasper, P. Rogl, H. Flandorfer, T. Cichorek, R. Pietri, and B. Andraka, Phys. Rev. B **60**, 422 (1999).
[36]B. Cornut and B. Coqblin, Phys. Rev. B **5**, 4541 (1972).
[37]F. C. Ragel, P. de V. du Plessis, and A. M. Strydom, J. Phys. Chem. Solids **71**, 1694 (2010).
[38]R. S. Shankland, *Atomic and Nuclear Physics*, 2nd ed. (Macmillan, New York, 1960).
[39]B. L. Drake, C. Capan, J. Y. Cho, Y. Nambu, K. Kuga, Y. M. Xiong, A. B. Karki, S. Nakatsuji, P. W. Adams, D. P. Young, and J. Y. Chan, J. Phys. Condens. Matter **22**, 066001 (2010).
[40]Y. Cheng, E. Ma, and H. Sheng, Phys. Rev. Lett. **102**, 245501 (2009).
[41]D. F. Brewer, *Progress in Low Temperature Physics* (North-Holland, Oxford, 1978).
[42]A. Tari, *The Specific Heat of Matter at Low Temperatures* (Imperial College Press, Cambridge, 1997).
[43]B. Huang, H. Y. Bai, and W. H. Wang, J. Appl. Phys. **110**, 123522 (2011).
[44]J. L. Finney, Proc. R. Soc. London, Ser. A **319**, 479 (1970).
[45]T. Egami, J. Mater. Sci. **13**, 2587 (1978).
[46]K. Yoshimura, T. Kawabata, N. Sato, N. Tsujii, T. Terashima, C. Terakura, G. Kido, and K. Kosuge, J. Alloys Compd. **317**, 465 (2001).
[47]Y. F. Yang, Z. Fisk, H. O. Lee, J. D. Thompson, and D. Pines, Nature **454**, 611 (2008).
[48]D. P. Rojas, J. Rodríguez Fernández, J. I. Espeso, and J. C. Gómez Sal, J. Alloys Compd. **502**, 275 (2010).
[49]L. E. De Long, R. W. McCallum, W. A. Fertig, M. B. Maple, and J. G. Huber, Solid State Commun. **22**, 245 (1977).
[50]P. W. Anderson, Phys. Rev. **109**, 1492 (1958).
[51]P. W. Anderson, Rev. Mod. Phys. **50**, 191 (1978).
[52]D. Ma, A. D. Stoica, X. L. Wang, Z. P. Lu, B. Clausen, and D. W. Brown, Phys. Rev. Lett. **108**, 085501 (2012).
[53]W. H. Wang, Nature Mater. **11**, 275 (2012).
[54]G. Li, Y. Y. Wang, P. K. Liaw, Y. C. Li, and R. P. Liu, Phys. Rev. Lett. **109**, 125501 (2012).
[55]Y. Li, P. Yu, and H. Y. Bai, J. Appl. Phys. **104**, 013520 (2008).
[56]K. Binder, Rev. Mod. Phys. **58**, 801 (1986).
[57]Q. Luo and W. H. Wang, J. Non-Cryst. Solids **355**, 759 (2009).